SAND80-0011
Unlimited Release
UC-62

Performance Testing of the FMC Fresnel-Belt Concentrating Solar Collector

Vernon E. Dudley, EG&G Inc.
Robert M. Workhoven

Prepared by Sandia Laboratories, Albuquerque, New Mexico 87185
and Livermore, California 94550 for the United States Department
of Energy under Contract DE-AC04-76DP00789

Printed January 1980

Sandia Laboratories

2900 Q(7-73)

Issued by Sandia Laboratories, operated for the United States Department of Energy by Sandia Corporation.

Printed in the United States of America

Available from
National Technical Information Service
U. S. Department of Commerce
5285 Port Royal Road
Springfield, VA 22161

Price: Printed Copy **$4.50** ; Microfiche $3.00

SAND80-0011
Unlimited Release
Printed January 1980

PERFORMANCE TESTING OF THE FMC FRESNEL-BELT CONCENTRATING SOLAR COLLECTOR

Vernon E. Dudley
Energy Measurements Group
EG&G, Inc.

Robert M. Workhoven
Experimental Systems Operations Division 4721
Sandia Laboratories
Albuquerque, NM 87185

ABSTRACT

This report summarizes the results of tests performed on the FMC Fresnel-Belt Solar Collector at the Midtemperature Solar Systems Test Facility. Tests were conducted over a temperature range from 100 to 250°C. Test objectives are defined, test procedures are described, and test results and conclusions are given.

CONTENTS

	Page
Introduction	5
Test Objective	5
Collector Description	5
Test Facility Description	9
Performance Test Definitions	13
Test Results	15
Summary of Results and Conclusions	26
References	29

ILLUSTRATIONS

Figure		
1.	FMC Fresnel-Belt Solar Collector	6
2.	Mirror Facets on the Flexible Belt	7
3.	Optical Geometry of the FMC Fresnel Belt	8
4.	FMC Cavity Receiver Cross Section	10
5.	Conceptual Design for a Long Row of Fresnel-Belt Collectors	11
6.	Data Printout for Efficiency Test	12
7.	Data Printout for Thermal Loss Test	12
8.	FMC Fresnel-Belt Efficiency Evaluation at 151^{o}C Input	16
9.	FMC Fresnel-Belt Efficiency Evaluation at 242^{o}C Input	17
10.	FMC Fresnel-Belt Efficiency Evaluation at 106^{o}C Input	18
11.	FMC Fresnel-Belt Efficiency Evaluation at 103.1^{o}C Input	19
12.	FMC Fresnel-Belt Efficiency Evaluation at 192.3^{o}C Input	20
13.	FMC Fresnel-Belt Efficiency Evaluation at 247.3^{o}C Input	21
14.	FMC Fresnel-Belt Efficiency vs Output Temperature	23
15.	FMC Fresnel-Belt Efficiency vs Delta Temperature/Insolation	24
16.	FMC Fresnel-Belt Receiver Thermal Loss	25
17.	Light Missing FMC Receiver	27
18.	Deformed Light Pattern	27

TABLES

Table		
1	FMC Collector Efficiency Test Data	22
2	FMC Collector Thermal Loss Data	26

PERFORMANCE TESTING OF THE FMC FRESNEL-BELT CONCENTRATING SOLAR COLLECTOR

Introduction

A series of concentrating solar collector designs are being tested at the Collector Module Test Facility (CMTF), located at the Sandia Laboratories in Albuquerque, New Mexico. The CMTF is a part of the Midtemperature Solar Systems Test Facility (MSSTF) at Sandia Laboratories. These facilities are operating as a result of a Department of Energy (DOE) program to characterize selected collector modules for possible future use in commercial energy systems (the program plan is contained in Reference 1).

The FMC Fresnel-Belt Solar Collector system is one of several unusual designs funded by the DOE to investigate possible advantages or disadvantages relative to the more common parabolic trough collectors.

Test Objective

Test objective for this test series was definition of performance characteristics of the FMC Fresnel-Belt Collector for fluid temperatures from 100 to 300^{o}C.

Collector Description

The Fresnel-Belt Solar Collector was developed and built by the Engineered Systems Division of the FMC Corporation, Santa Clara, CA. Figure 1 is a photograph of the collector at the CMTF. The design uses an endless belt with a Fresnel reflecting surface to reflect light into a fixed receiver. A baseplate supports the belt so that the basic belt surface becomes a section of a cyclinder. This geometry provides a 30^{o} rim angle, with a focal length equal to the radius of the cylindrical surface. The motion of the belt sliding over the baseplate is nearly the optical equivalent of rotating a parabolic mirror about the cylindrical axis, thus allowing the focal line from the reflector surface to be maintained on a fixed receiver located at the axis of the cylinder.

Figure 2 illustrates the placement of the narrow mirror facets that make up the Fresnel reflector surface of the moving belt. The individual mirror strips on the test model are 1.27 cm wide and 61 cm long. Three of these long, narrow mirror strips placed end-to-end make up the total 183 cm width of the mirror surface. Each glass mirror facet has a front-surface aluminized reflective coating, Type CR-H001, applied by Optical Coating Laboratories, Inc. Reflectivity of these mirror facets was 95% when new. Each facet is fixed to the belt substrate at a different facet angle such that all facets reflect incoming sunlight into the receiver.

A polyurethane material, Isoflex 517, was used to support the mirror facets on the stainless-steel belt. The glass mirror facets were bonded to the polyurethane with Chem Lok 518.

Figure 3 illustrates the overall optical geometry of the FMC Fresnel-reflector system. Incoming light is nearly parallel as it intersects the cylindrical reflector surface. Individual mirrors are mounted on this surface such that each is perpendicular to a point in space called the mirror normal. The basic cylindrical surface is positioned so that the receiver is located at the center of the radius of curvature. If the reflector surface is rotated about the center such that the plane containing the receiver and the mirror normal also includes the sun, all the mirror facets reflect light into the receiver aperture.

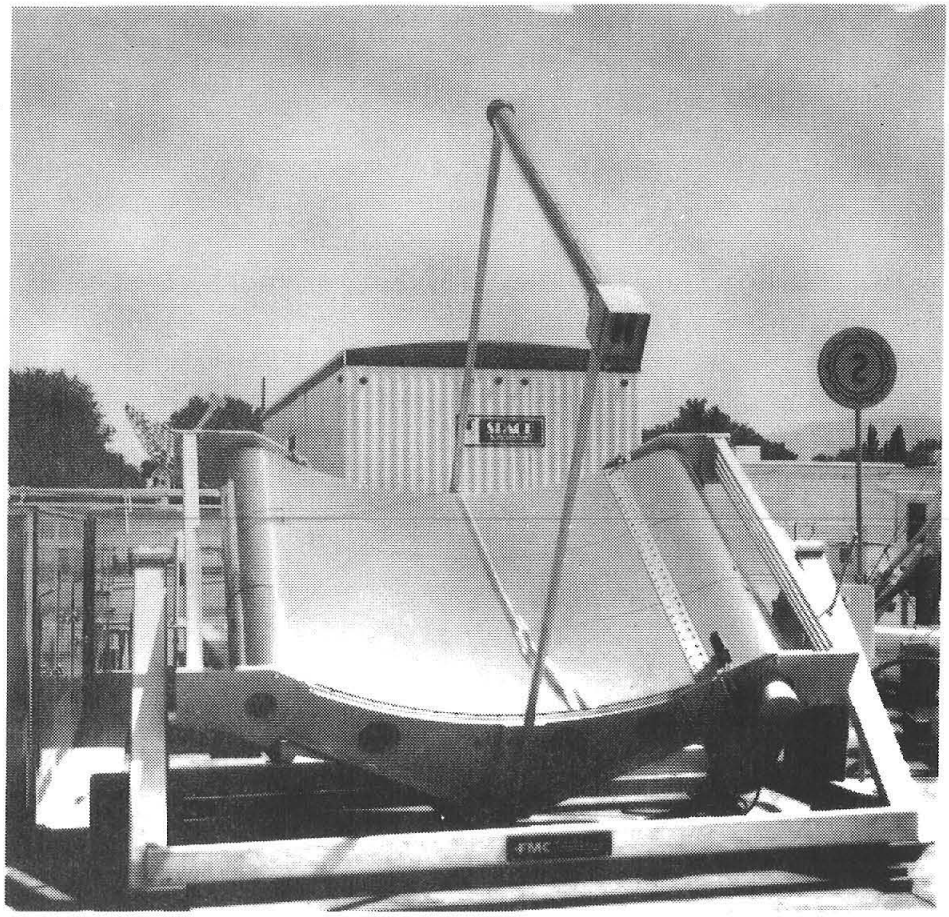

Figure 1. FMC Fresnel Belt Solar Collector.

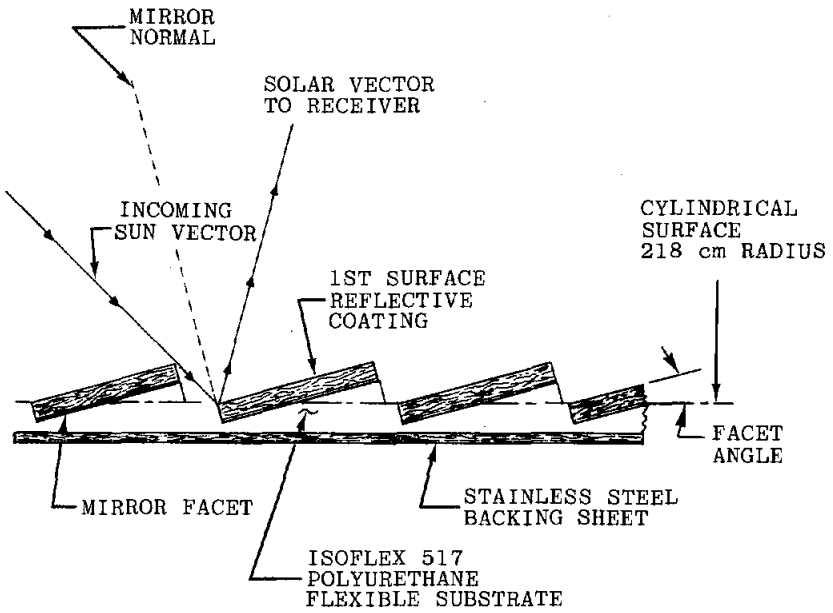

Figure 2. Mirror Facets on the Flexible Belt.

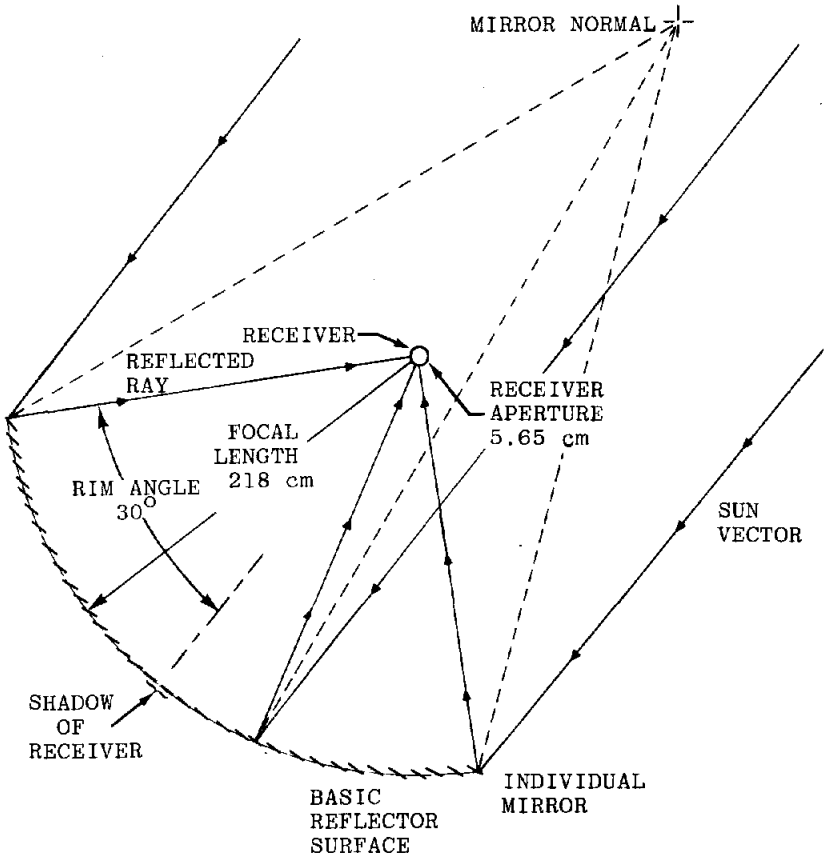

Figure 3. Optical Geometry of the FMC Fresnel-Belt.

Figure 4 is a cross section of the receiver used on the FMC collector prototype. All 10 of the 0.95 cm diameter absorber tubes are connected in series, and have a black-chrome, solar spectrum selective surface plating. A thin stainless-steel shield on the nonilluminated side reduces radiation loss from the absorber tubes. Receiver end plates were sealed to the glass envelope so that a vacuum could be maintained inside the receiver to minimize thermal losses.

Total optical aperture of the collector was only 4 m^2; average concentration ratio of sunlight on the absorber surfaces was about 16.2.

Because of the short length of the collector's receiver axis it was not feasible to test with the longitudinal axis oriented east-west. The flexible belt and receiver assembly were delivered on a heavy frame which oriented the receiver axis north-south, and provided an adjustable north-south tilt angle. The tilt angle was adjusted during the tests to provide a zero incidence angle at solar noon. This arrangement would not be suitable for a large collector field; it was used for test purposes only.

Figure 5 shows a conceptual design for a long row of 45° rim angle, east-west axis solar collectors using the Fresnel-belt principle. Such a collector could be installed with either an east-west or north-south axis.

Sun tracking of the FMC Fresnel-belt was accomplished with a Delevan shadow-band sun sensor mounted on the flexible belt. Drive power was supplied by a variable speed drive motor through Harmonic Drive speed reducers.

Further details of the development and construction of the FMC Fresnel-belt collector are contained in Reference 2.

Test Facility Description

The fluid loop used for this test series was Fluid Loop 1, which is designed to supply Therminol-66 as a heat transfer fluid at temperatures from 100 to $330^{\circ}C$. Design flow rates available in this loop range from 0.4 to 40 L/min.

Each test day began by heating the fluid loop with electric heaters to the desired collector input temperature. Usually only one temperature point was attempted in one day because of the time required for temperature stabilization. The collector system was placed in focus as early as possible each day so that recovered solar heat could aid in reaching the desired temperature. Because of the small aperture area of the FMC collector, another larger collector was operated in parallel to increase the solar heat recovery. For each test, input temperature and flow-rate were maintained constant while output temperature varied according to test conditions.

The flow-rate of the heated Therminol-66 through the system was measured with a turbine flowmeter. A calibrated copper constantan thermocouple was installed at each end of the collector to determine temperatures into and out of the receiver. These two thermocouples, one from each end of the absorber tube, were also connected as a differential pair to determine the delta temperature for calculations of heat gain or loss. Direct solar radiation was measured with an Eppley NIP pyrheliometer. Receiver differential pressure, ambient temperature, wind direction, and windspeed measurements completed the active data collection.

Data provided by the instruments described above are converted to a digital format by an analog-to-digital data system. A minicomputer processed the data and critical data for the test being performed are printed. Figures 6 and 7 are copies of the printed data from an efficiency test and from a thermal loss test, respectively.

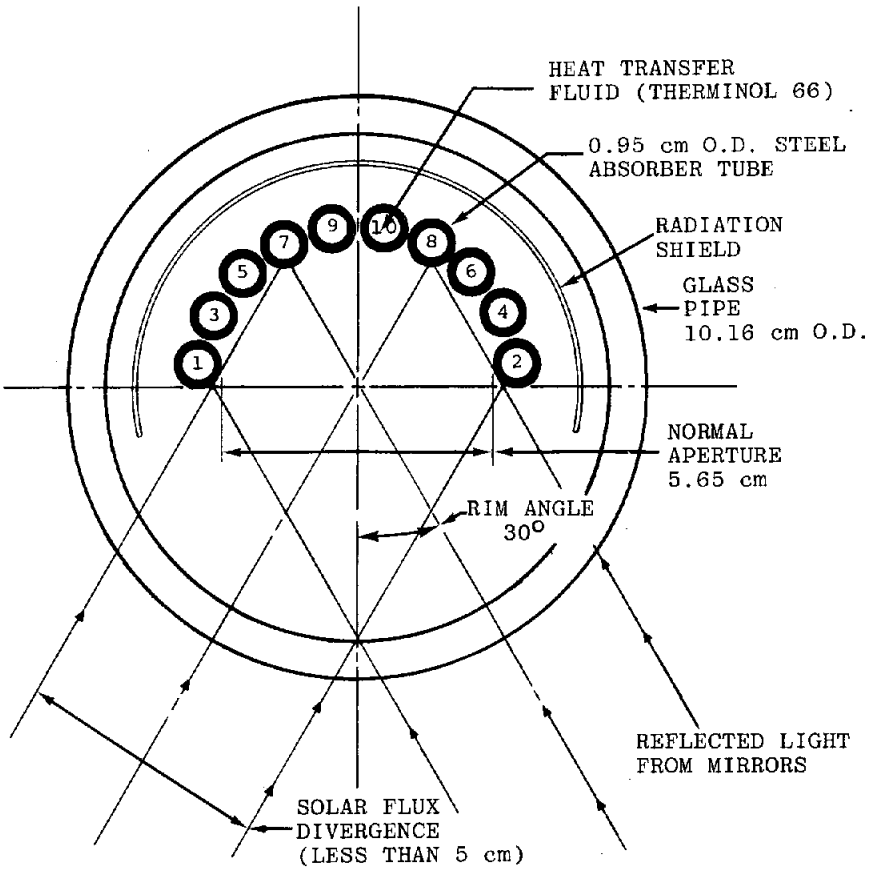

Figure 4. FMC Cavity Receiver Cross Section.

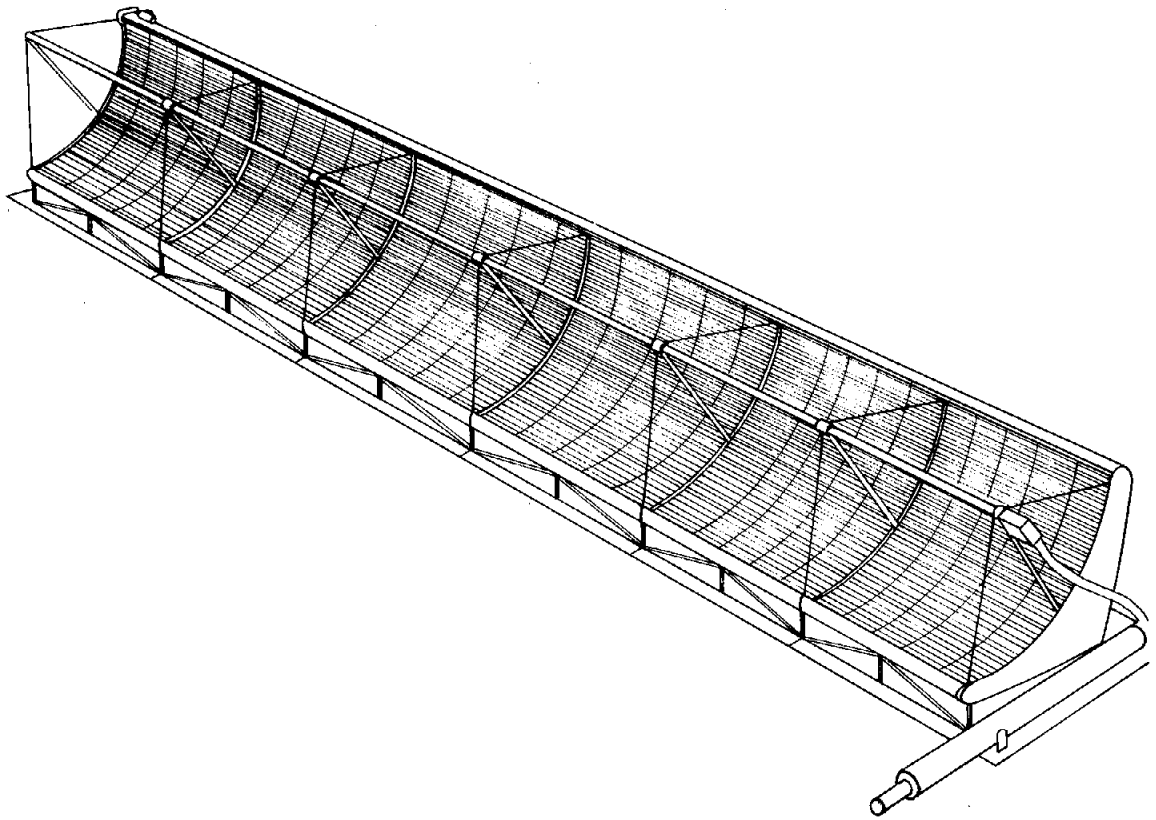

Figure 5. Conceptual Design for a Long Row of Fresnel-Belt Collectors.

♦♦♦ FMC FRESNEL BELT EFFICIENCY TEST ♦♦♦

TEST DATE: 12 JUNE HOUR 12 MINUTE 45 (SOLAR TIME)

27.44	(DEG C)	AMBIENT TEMPERATURE	(DEG F)	81.39
214	(DEGREES)	WIND DIRECTION		
.1	(M/SEC)	WIND SPEED	(MPH)	.3

TEMP IN	TEMP OUT	SOLAR WATTS/M^2	DELTA TEMP	FLOW LITERS/MIN	EFFICIENCY PERCENT
192.22	200.5	1005.4	8.25	4.42	29.1
192.28	200.56	1007.2	8.27	4.45	29.3
192.28	200.61	1007.1	8.31	4.42	29.3
192.28	200.61	1006.1	8.33	4.44	29.5
192.28	200.61	1005	8.33	4.42	29.4
192.22	200.61	1004.4	8.35	4.44	29.6
192.28	200.61	1005.1	8.33	4.42	29.4
192.28	200.61	1005.2	8.29	4.42	29.3
192.22	200.56	1005.1	8.31	4.41	29.3
192.28	200.61	1005.4	8.27	4.41	29.1
		10 POINT AVERAGES			
192.262	200.589	1005.6	8.304	4.425	29.33

Figure 6. Data Printout for Efficiency Test.

♦♦♦ FMC FRESNEL BELT THERMAL LOSS TEST ♦♦♦

TEST DATE: 12 JUNE HOUR 15 MINUTE 36 (SOLAR TIME)

32.72	(DEG C)	AMBIENT TEMPERATURE	(DEG F)	90.9
219	(DEGREES)	WIND DIRECTION		
.2	(M/SEC)	WIND SPEED	(MPH)	.4

TEMP IN	TEMP OUT	DELTA TEMP	FLOW LITERS/MIN	WATTS GAIN/LOSS
192.89	191.44	-1.41	4.54	-206.9
192.94	191.44	-1.38	4.57	-203.9
192.94	191.44	-1.34	4.57	-198
192.89	191.44	-1.39	4.56	-204.9
192.89	191.44	-1.36	4.59	-201.8
192.83	191.44	-1.3	4.55	-191.2
192.89	191.44	-1.34	4.56	-197.5
192.89	191.44	-1.34	4.56	-197.5
192.89	191.39	-1.36	4.56	-200.5
192.89	191.39	-1.36	4.56	-200.5
		10 POINT AVERAGES		
192.894	191.43	-1.358	4.562	-200.369

Figure 7. Data Printout for Thermal Loss Test.

Unless otherwide labeled, temperatures cited in those figures are in degrees Celsius. The delta temperature shown in both figures is not the arithmetic difference of the input and output temperatures but is obtained by a separate, independent computation from the output signal of the paired differential thermocouples.

The speed of the data system was such that all the data channels could be read, calculations performed, and a line in the data table printed in about 20 seconds. The average values were automatically printed after 10 data points were accumulated. The complete data printout as shown in Figures 6 and 7 was repeated at intervals of about 3-4 minutes throughout a test run. Thirty-two measured and calculated data values from the data system were recorded on magnetic tape every 20 seconds. Only those shown in Figure 6 or 7 were printed in real time. The number of decimal places that are printed in Figures 6 and 7 should not be taken as indicating the accuracy of the data system since the choice of the print format was dictated by the peculiarities of the computer system. Either a loss or an efficiency data print was made continuously when the system was operating; however, only those data blocks occurring under stable conditions are included in this report.

Performance Test Definitions

For each data set during a test run, the specific heat and the density of the Therminol-66 are calculated. The properties of Therminol-66 used for these calculations are taken from Reference 3. Heat gain (loss) is then computed from the following formula:

$$Q = \dot{m} C_p \Delta T$$

in which

Q = heat gain, kJ/h
$\dot{m}$ = mass flow-rate of fluid, kg/h
C_p = specific heat of fluid, kJ/kg^{o}C
ΔT = in/out temperature differential, ^{o}C

A successful loss measurement was one in which the values for input and output temperatures remained constant to within 0.1^{o}C or less. Loss tests were conducted with the mirror belt sufficiently defocused so that no light from the mirror would strike any part of the receiver tube assembly.

On most days, efficiency measurements were made from 2 hours before noon to about 2 hours after noon. The mirror system in this prototype could not be focused on the receiver at times more than about 2 hours from solar noon. Loss measurements were made for about 2 hours after completion of efficiency tests; the fluid loop was then placed in a cooling mode prior to shutdown for the day.

For an efficiency test, efficiency was calculated from the following formula:

$$\eta = \frac{Q/A}{I}$$

in which

η = solar collector efficiency
Q = heat gain, W
A = collector aperture area, m^2
I = direct solar radiation, W/m^2

A successful efficiency data point measurement consists of a least one of the 10 point averages during which input and output temperatures changed by 0.1^{o}C or less, flow rates varied by 0.1 L/min or less, delta temperatures remained within 0.1^{o}C,

and solar radiation remained constant to about 1%. Temperatures, flow-rate and insolation had to have been nearly as stable as described above for at least 5 to 10 minutes prior to the measurement; otherwise that data point was not considered to be a reliable measurement. Efficiency measurements are normally made with insolation greater than about 900 W/m^2.

The temperature, flow-rate and insolation stability criteria outlined above are necessary because the heat gain formula given assumes steady-state conditions. If near steady-state conditions can be achieved during a collector test, the computed values for heat gain (or loss) and efficiency will be nearly constant also, with some scatter in the data due to noise. Because of the thermal mass of the collector system, any change in temperature, flow-rate or insolation will result in measurements that do not correctly represent the performance of the collector.

Even on a sunny day that appears ideal for testing a solar collector, there are still variations in solar radiation. However, these variations can be relatively small, as can be seen in several of the test data plots later in this report. Small, rapid variations of this kind produce scatter in the efficiency data, but no long-term systematic errors.

As operated at the CMTF, the heat-transfer fluid supply loop tends to produce fluid flow-rate variations similar to those seen in the solar radiation input--small, rapid fluctuations with no long-term trend towards a higher or lower rate. These variations also produce scatter in the measured data.

Small, rapid temperature fluctuations also appear in the measured data, again producing data scatter. However, the temperature measurements are also subject to fairly long-term, slow changes which can result in fairly large, systematic errors in heat gain/loss and efficiency calculations. One typical source of this kind of temperature drift is the constantly increasing temperature that occurs each test day as the system is heated towards the intended operating temperature. Another is the temperature decay that continues for very long times after the collector system is defocused to begin a thermal loss test.

At the CMTF, collector input and output temperatures are usually measured less than one second apart in time. However, the fluid whose temperature is being measured at the collector input may not arrive at the collector output for a relatively long time--from several seconds up to several minutes. Thus an efficiency, or heat gain/loss, measurement will not be valid unless the input and output temperatures are stable for at least as long as the transit time of the heat-transfer fluid through the system.

Because of the thermal mass of both the fluid supply system and the collector, stable temperatures must be held for relatively long periods of time before the complete system is in thermal equilibrium and valid measurements can be made. A small constant drift in temperatures can produce test data that looks quite acceptable; however, it contains a systematic error because of the thermal mass shift of in/out delta temperature. For example, with one collector tested, a constant temperature increase of $0.7^{\circ}C$ per minute produced an efficiency measurement that had a very small data scatter and a nearly constant efficiency value for more than an hour. This measured efficiency value turned out to be 5 percentage points lower than the efficiency measured later with more stable temperatures. In another case, with a collector system of greater thermal mass, a similar slow upward drift in input temperature produced an efficiency measurement 15 percentage points lower than the true value.

If the input temperature drift is towards lower temperatures, errors of similar magnitude result, but the measured efficiency will be greater than the value obtained under stable conditions.

The same problem as oulined above for an efficiency measurement also occurs during thermal loss measurements. The error in thermal loss from unstable temperatures is larger than the efficiency error because the receiver delta temperature during a loss test is usually much less than during an efficiency measurement.

The requirement for $0.1^{\circ}C$ stability in measured temperatures for a usable data point is empirically based. It appears to produce valid data, and is also about as good as the fluid loop and collector system can attain in the outdoor test environment.

Test Results

The FMC Fresnel-belt collector was delivered to the test site in April 1978; a backlog of collectors awaiting tests prevented installation on the fluid loop test pad until August 1978. Figure 8 shows a plot of direct solar radiation input and measured efficiency data that is quite scattered because of variations in the input temperature; input fluid line insulation was not yet in place during this test. The tests plotted in Figures 8, 9 and 10 were originally intended only to check out the collector and data system prior to beginning formal testing. They are shown here because they subsequently became important in determining the nature of a decrease in collector performance.

Figure 9 resulted from a similar test the following day. Operating temperature was nearly $250^{\circ}C$; the efficiency data was much more stable because inlet tubing insulation had been installed to assist in stabilizing input temperature.

Figure 10 was obtained from an efficiency test near $100^{\circ}C$. This low temperature test was intended to minimize thermal loss so as to obtain the maximum possible efficiency. Oscillations and dips in the efficiency curve were caused by collector tilt adjustments and experimentation with the sun tracking device.

Note the characteristic curved shape of the efficiency plots in Figures 8, 9 and 10. This shape results from changes in the incidence angle of incoming solar radiation. The collector was tilted to achieve a 0° incidence angle at solar noon; as the sun's elevation changed with time, end losses and cosine effects caused the recovered energy to decrease for times before and after solar noon. For the tilt angle used, this drop in efficiency and energy recovery should be symmetrical with time about solar noon, as can be seen in the 3 preceding plots. Because of the relatively narrow 30° rim angle, combined with the north-south mount, data on this prototype collector could be taken only one hour 50 minutes either side of solar noon.

Testing of the FMC collector was not continued to completion in September 1978 because of higher priority testing being conducted at the same time; testing could not be resumed until June 1979.

Figure 11 was obtained on June 6, 1979 at the same $112^{\circ}C$ operating temperature used for the test plotted in Figure 10. A comparison of these two figures make it apparent that something drastic had happened to the collector in the time between the two tests: the basic shape of the efficiency curve is different, and the efficiency has decreased about 20 points, from 51% to 31%.

Testing continued while a search was made for the cause of such a large decrease in performance. Figures 12 and 13 were obtained at temperatures near $200^{\circ}C$ and $250^{\circ}C$

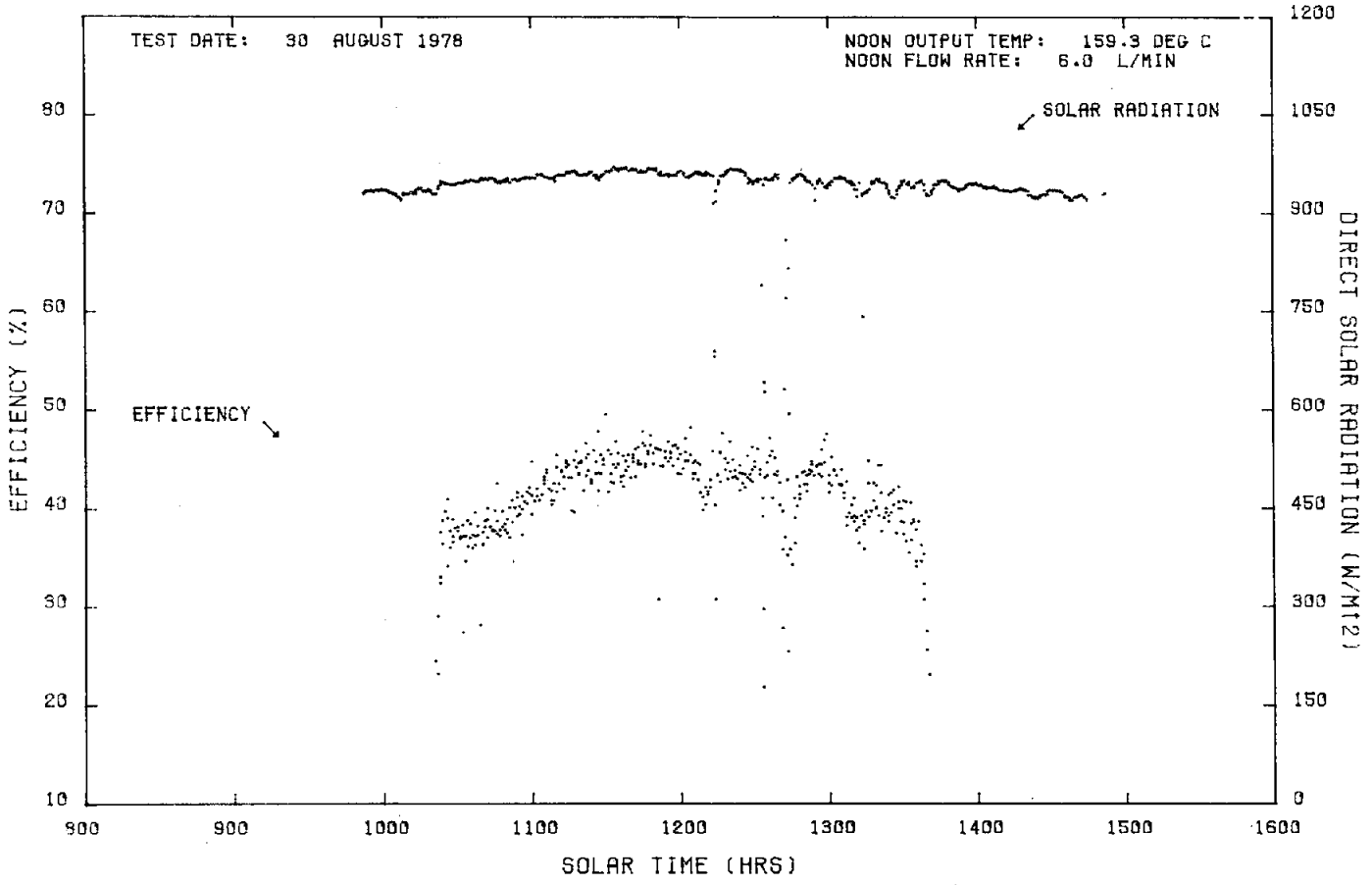

FIGURE 8 FMC FRESNEL BELT EFFICIENCY EVALUATION AT 151 DEG C INPUT

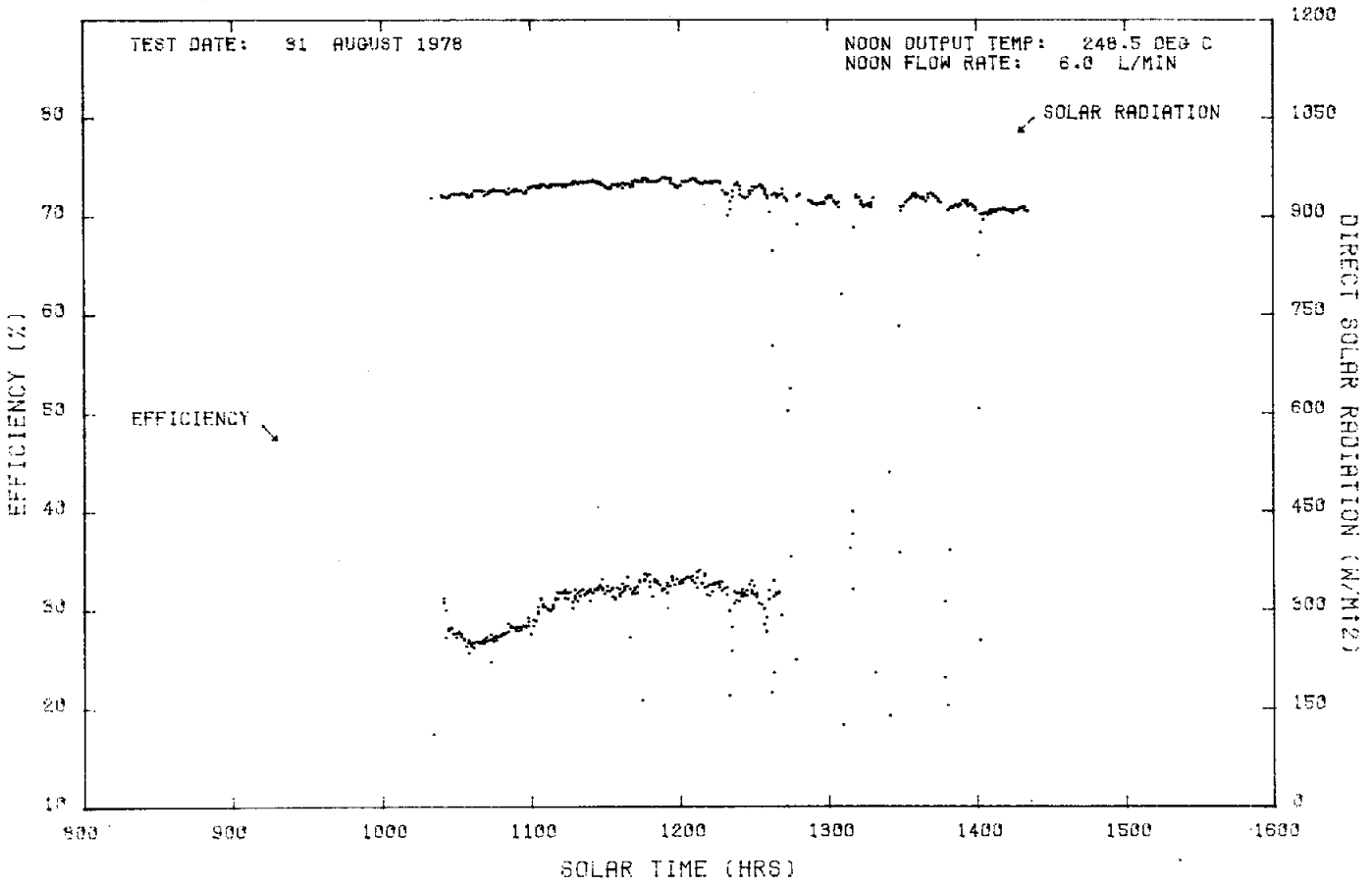

FIGURE 8 FMC FRESNEL BELT EFFICIENCY EVALUATION AT 242 DEG C INPUT

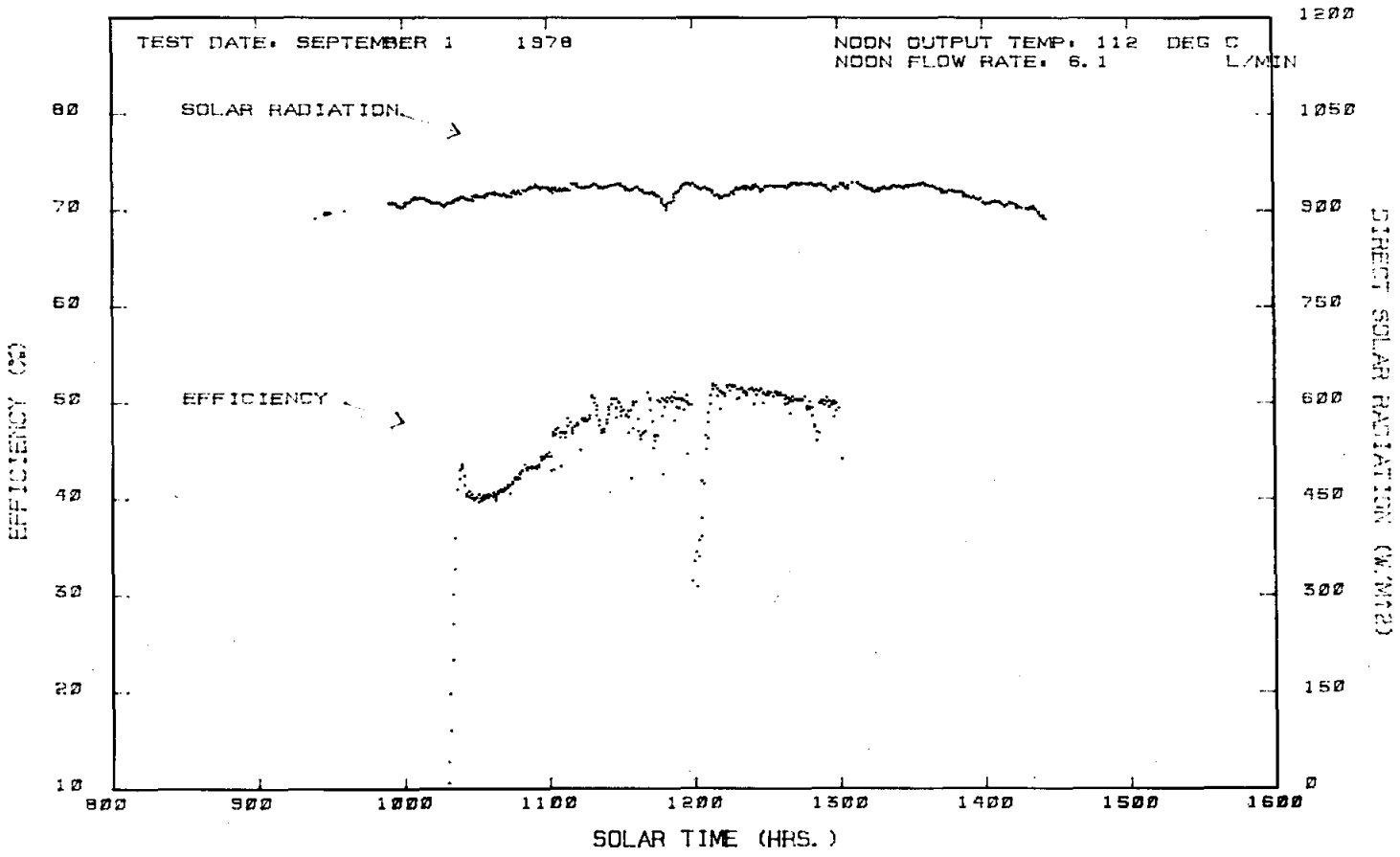

FIGURE 10 FMC FRESNEL BELT EFFICIENCY EVALUATION AT 106 DEG C INPUT

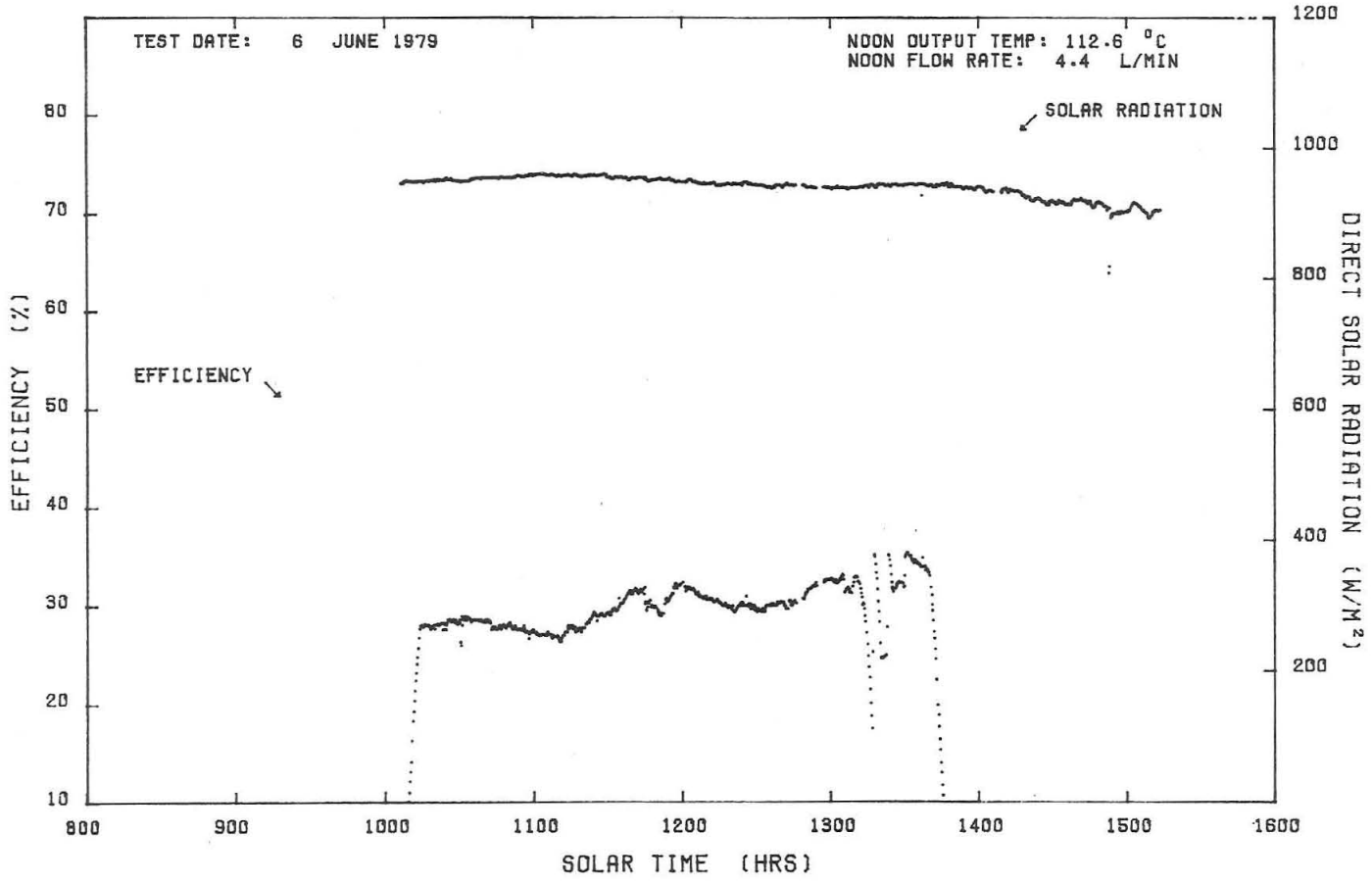

FIGURE 11 FMC FRESNEL BELT EFFICIENCY EVALUATION AT 103.1 °C INPUT

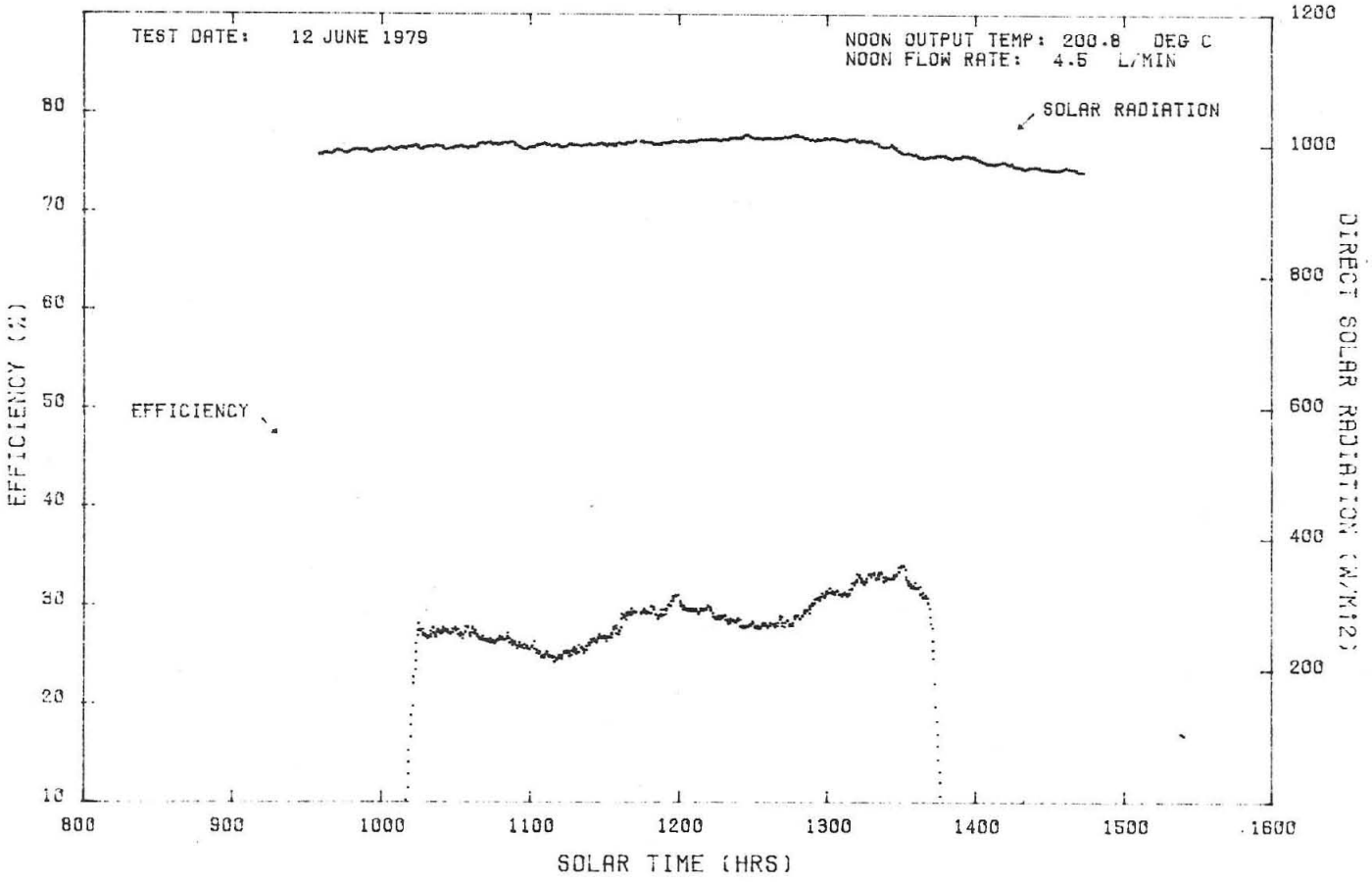

FIGURE 12 FMC FRESNEL BELT EFFICIENCY EVALUATION AT 192.3 DEG C INPUT

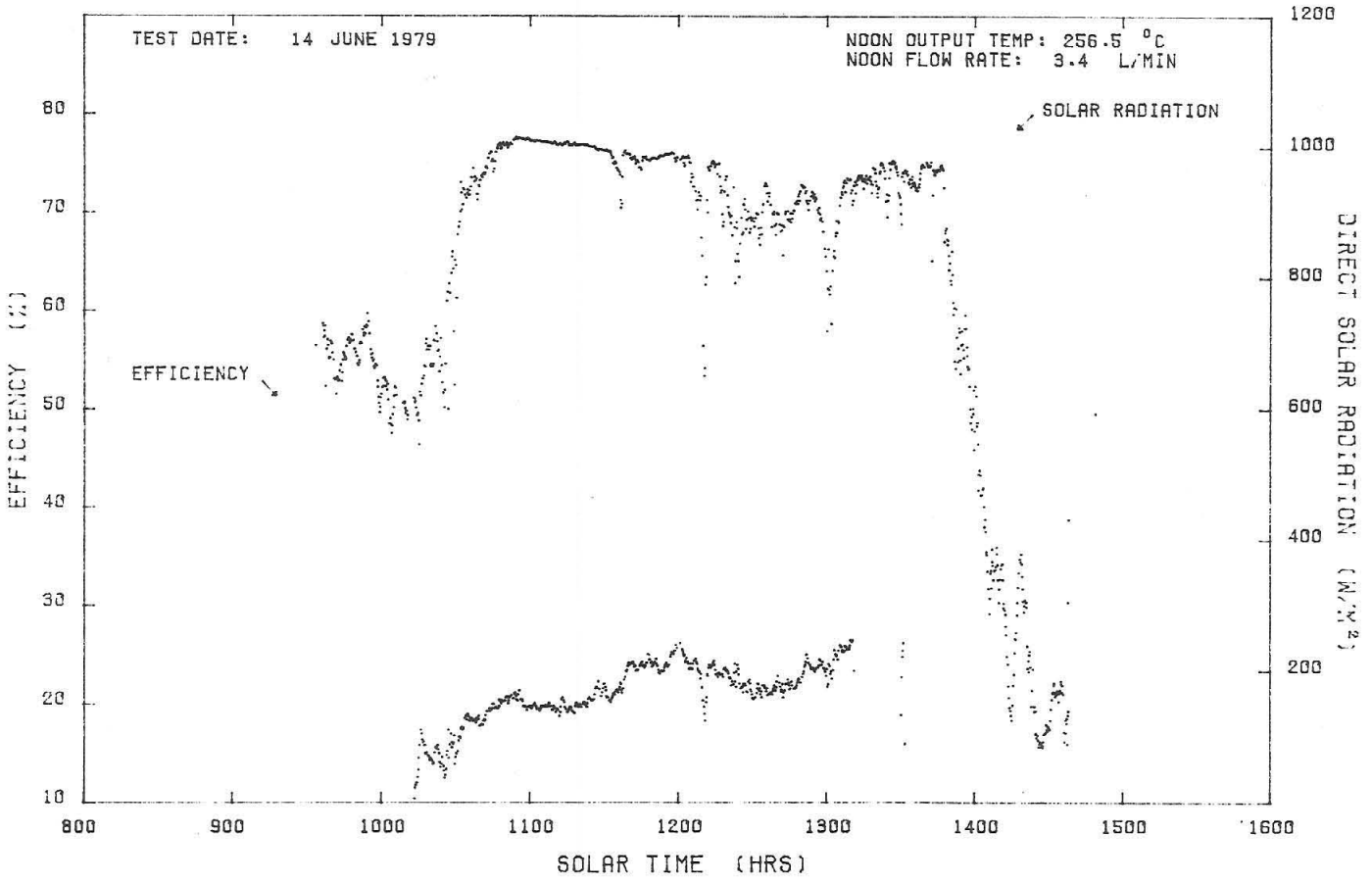

FIGURE 13 FMC FRESNEL BELT EFFICIENCY EVALUATION AT 247.3 °C INPUT

respectively. Both confirmed the loss of efficiency and repeated the odd shaped efficiency curve. June 14 (Figure 13) was not an ideal test day; intermittent clouds drifted across the test site during the early morning and became heavier after noon.

Tests were also conducted with a vacuum inside the glass receiver envelope. The desired vacuum could not be attained because of air leaks into the receiver; the receiver was removed and disassembled for resealing without completely correcting the leaks. About 0.2 torr was the best vacuum that could be achieved.

Table 1 contains the data obtained during the efficiency tests; Figure 14 is a plot of the efficiency data. Three curves are shown in Figure 14; one resulting from the original tests of September 1978, another from data obtained 10 months later, in June 1979, and an abbreviated range of temperatures showing an improvement of about 3 percentage points resulting from a receiver vacuum of about 0.2 torr.

Table 1. Efficiency Data for FMC Fresnel-Belt Collector

Test Date	Insolation (W/m^2)	Temperature Out (^oC)	Receiver ΔTemp (^oC)	Flow Rate (L/min)	Efficiency (%)
8/29/78	940	203.1	7.8	6.29	42.1
8/30/78	963	159.3	9.4	5.97	45.2
8/31/78	958	248.5	7.3	6.02	38.3
9/01/78	939	115.9	10.5	6.10	50.5
9/05/78	966	164.0	9.0	6.04	43.9
9/06/78	940	115.4	10.3	6.05	49.4
6/06/79	951	112.6	9.4	4.38	31.8
6/07/79	924	245.0	6.4	3.79	21.8
6/11/79	1036	205.5	10.6	3.39	27.8
6/12/79	1006	200.9	8.4	4.54	30.7*
6/14/79	980	255.8	8.9	3.36	25.2*
6/15/79	955	191.0	10.5	3.41	29.7*

*Receiver Vacuum - Approximately 0.2 torr

Figure 15 is the same efficiency data plotted as a function of $\Delta T/I$ (average receiver temperature minus ambient temperature, divided by direct solar radiation).

Table 2 contains data obtained during thermal loss testing of the FMC receiver. Figure 16 is a plot of the same data. The right ordinate in Figure 16 is total thermal loss, as measured. The left ordinate shows the thermal loss per unit area of collector aperture. Measurements confirmed that a receiver vacuum reduces the thermal loss, but too few points were obtained to plot a curve showing this change across the temperature range.

During the June 79 test series, several mirror strips were observed to have lost their bond to the flexible polyurethane substrate. None actually fell off the belt; they remained bonded along one edge, swinging as though on hinges. These loose mirrors were relatively few, and were fastened back in place so that their reflected light would not be lost. However, it soon became apparent that a larger number of mirrors were not firmly bonded in place over their whole undersurface. When the degraded collector performance became apparent, a closer look was taken at the mirrors and the flexible belt.

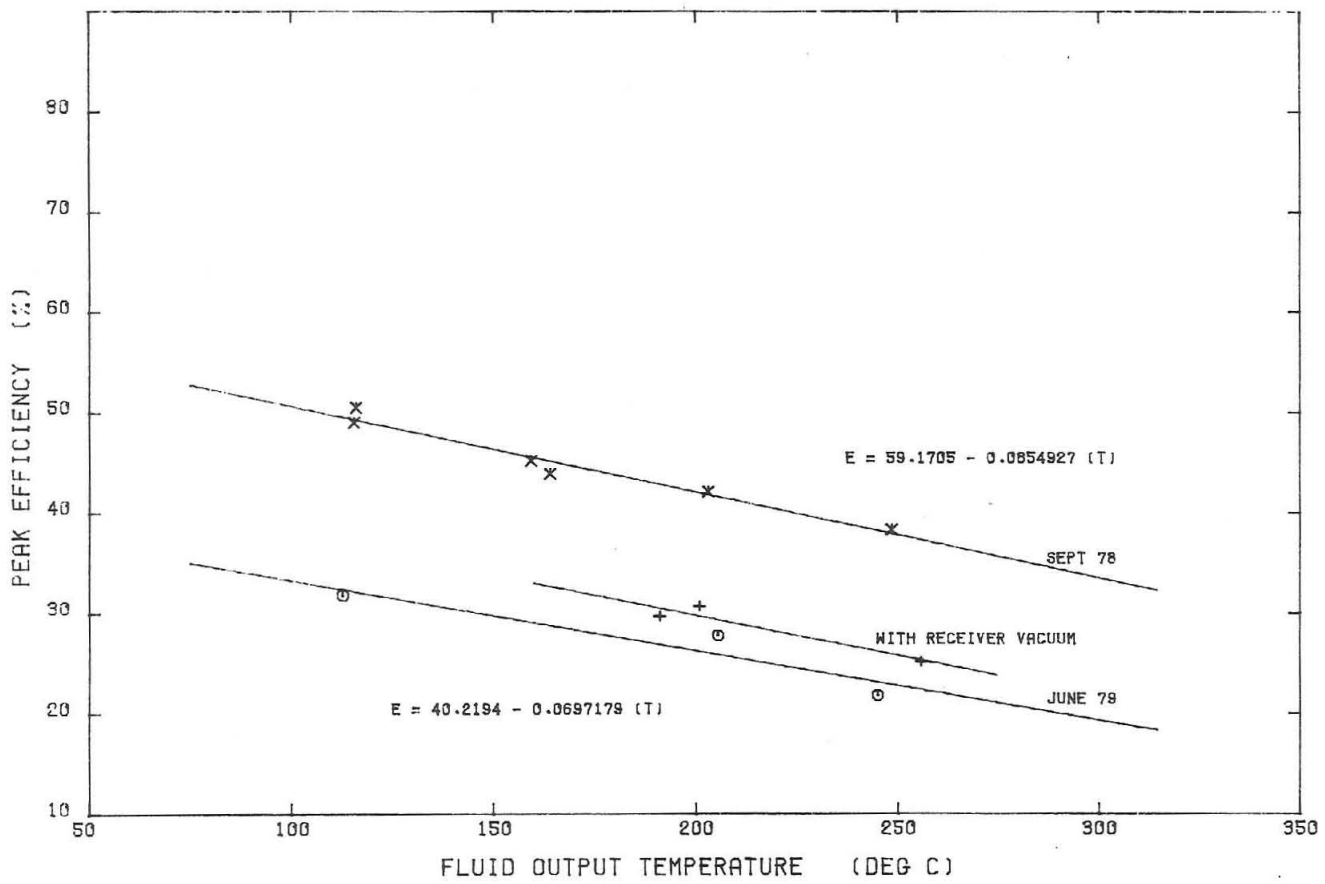

FIGURE 14 FMC FRESNEL BELT EFFICIENCY VS OUTPUT TEMPERATURE

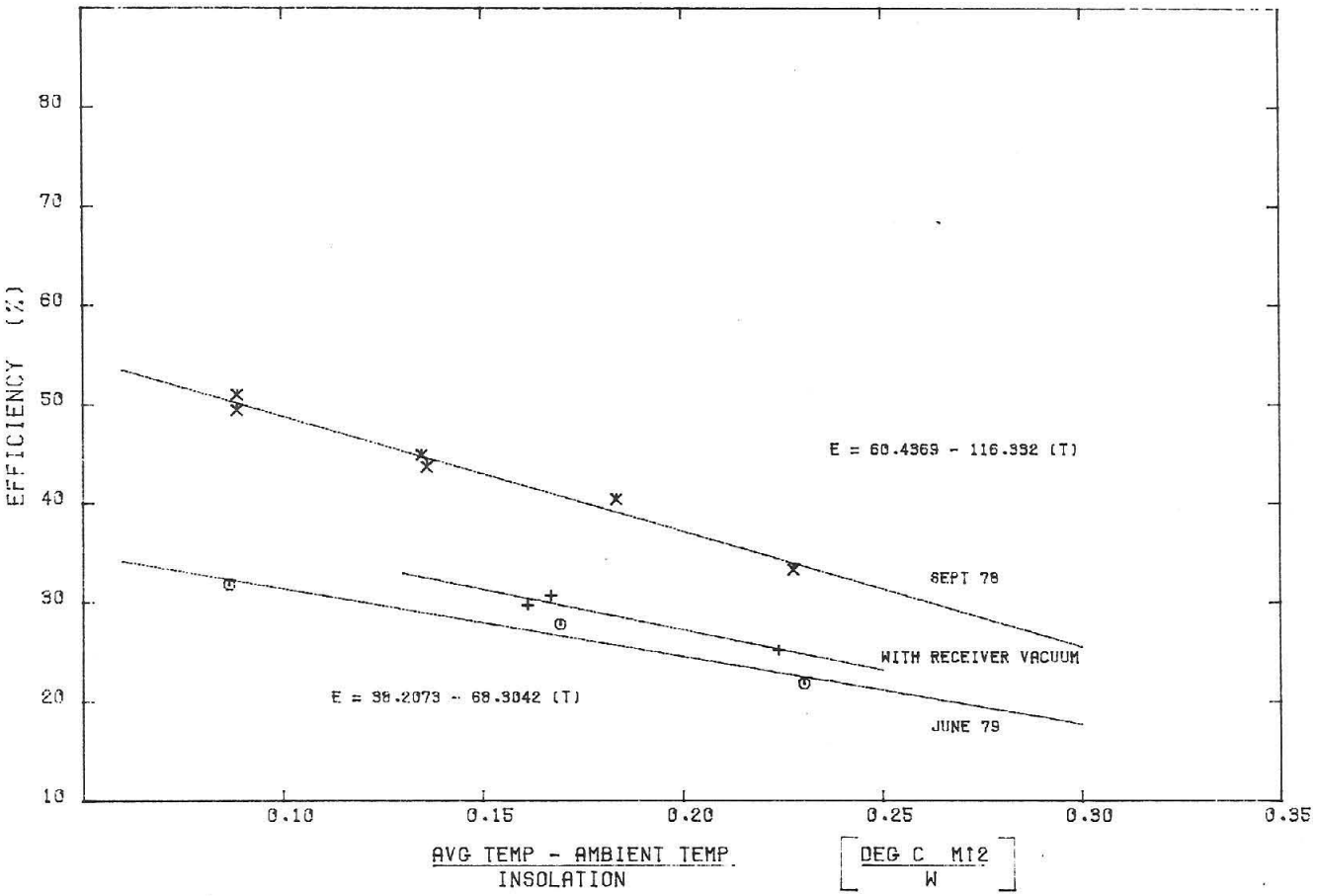

FIGURE 15 FMC FRESNEL BELT EFFICIENCY VS DELTA TEMPERATURE/INSOLATION

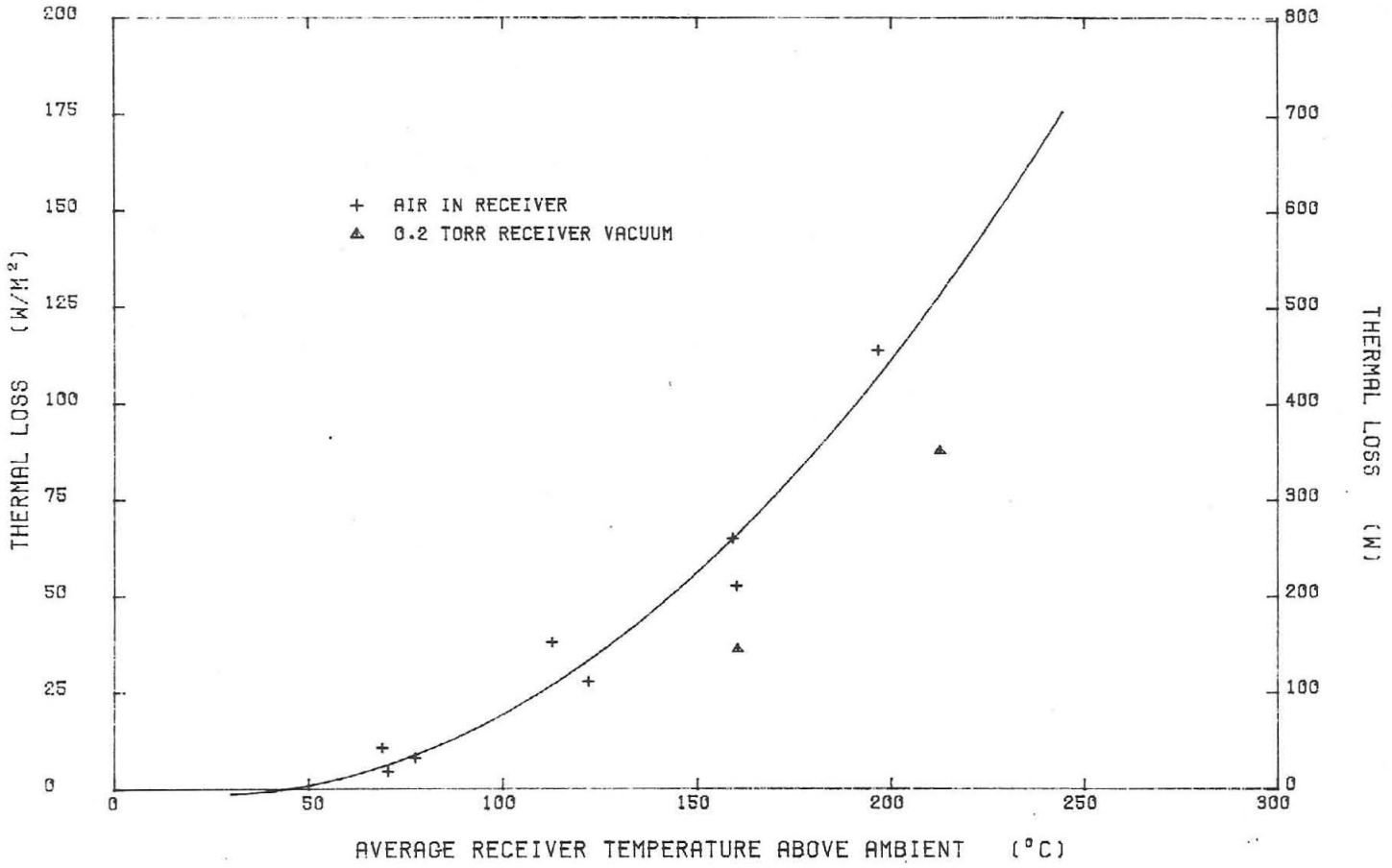

FIGURE 16 FMC FRESNEL BELT RECEIVER THERMAL LOSS

Table 2. FMC Collector Thermal Loss Data

Test Date	Insolation (W/m^2)	Average Temp Above Ambient (^oC)	Flow Rate (L/min)	Wind Speed (m/s)	Loss (W)
8/30/78	936	121.9	5.9	2.6	111.0
9/01/78	829	212.7	6.0	2.2	323.7
9/06/78	846	77.4	6.0	2.3	32.4
6/04/79	109	112.6	3.3	0.7	154.0
6/05/79	4.5	159.2	3.8	0.2	263.0
6/06/79	914	70.3	3.2	0.6	18
6/07/79	1	196.7	3.8	0.6	461.3
6/12/79	975	160.5	4.6	0.6	146.4*
6/12/79	964	160.1	4.6	0.2	213.3
6/14/79	973	212.7	3.4	0.3	355*

* 0.2 torr vacuum in receiver

Figure 17 is a photograph of a narrow board held across the collector aperture just above the receiver. Prior to taking the photograph, opaque black masks were placed across the ends of the mirror belt assembly so that only the active mirror surfaces could reflect light toward the receiver. Assuming perfect focus, all the mirror strips would place their reflected light within the 5.65 cm receiver aperture; none should miss the receiver to be seen on a surface placed across the receiver as in Figure 17.

A number of photographs were made at intervals across the width of the mirror; all were similar to Figure 17. The marks on the board in Figure 17 are spaced at ∿15-cm (6-inch) intervals. Light was found to be missing the receiver at distances up to ∿30-cm on each side. This scattered light is believed to be the reason for the collectors' degraded performance.

Debonded mirrors were not the only cause of scattered light. A number of the scattered spots were traced back to the mirrors responsible; they appeared to be still firmly bonded to the flexible polyurethane substrate. The polyurethane is flexible enough that slight finger pressure on the mirror surface can be seen to move the reflected light pattern.

Figure 18 shows the shape of some of the reflected light patterns that were falling outside the intended receiver aperture. The curved patterns show that the facet angle varied along the length of some of the mirror strips.

Measurements were made on several mirror segments to determine any loss of reflectivity from the first surface aluminized reflective coating. Reflectivities were about 90%; this slight degradation in reflectivity is not enough to contribute materially to the loss in measured efficiency.

Because of the degraded performance of the FMC collector, testing was terminated without completing tests over the design operating temperature range.

Summary of Results and Conclusions

Initial tests established the efficiency of the FMC Fresnel-belt collector at about 51% near 100°C, decreasing to about 35% near 300°C output temperatures. After about 16 months of outdoor exposure, and 10 months after the initial efficiency tests, the efficiency had degraded nearly 20 points, to near 32% at 100°C.

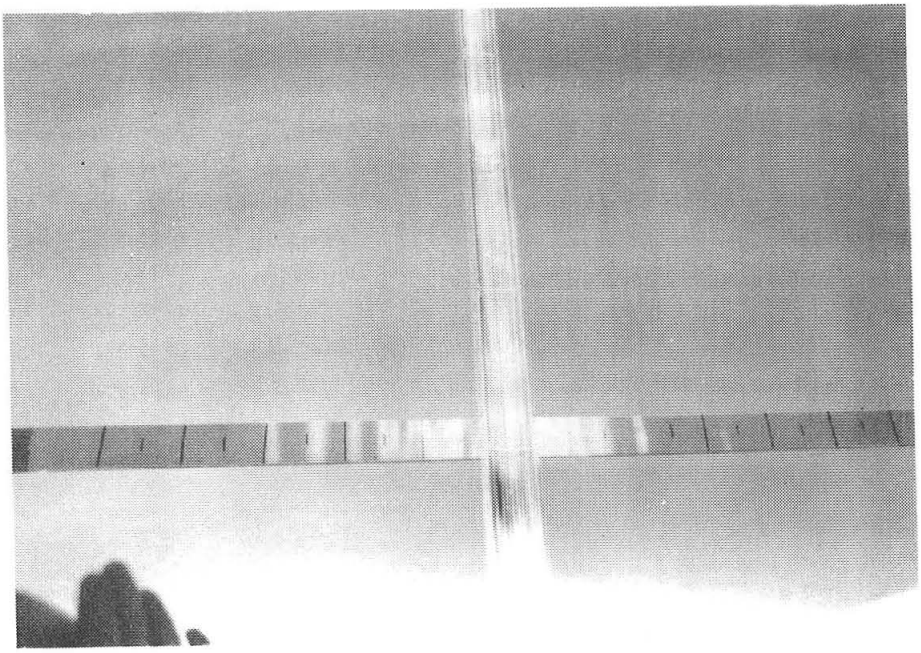

Figure 17. Light Missing FMC Receiver.

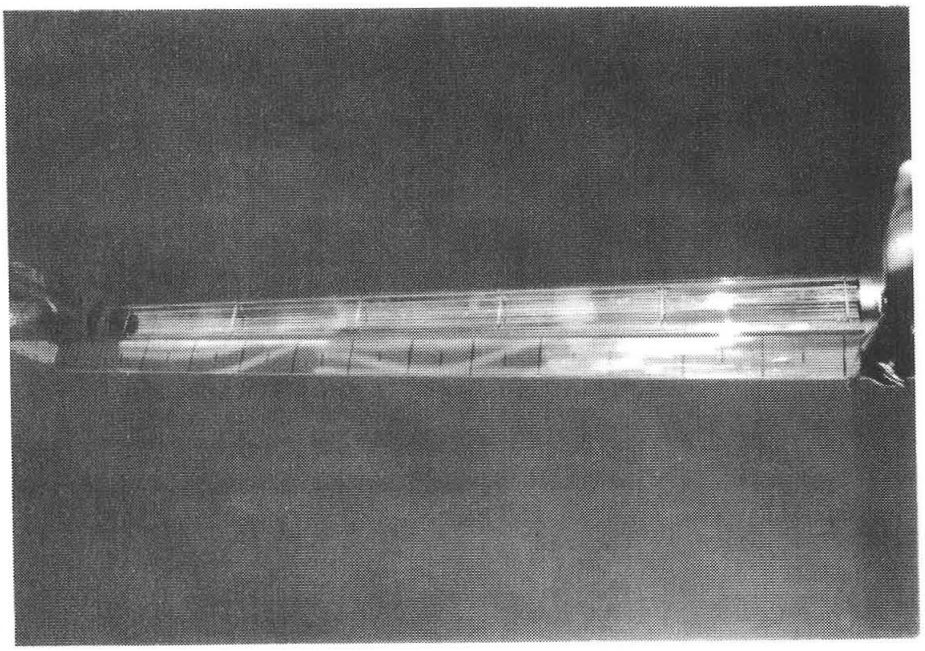

Figure 18. Deformed Light Pattern.

Unfortunately, the initial efficiency measurements were not made until after about 6 months of outdoor exposure, so it is not known if some degradation had occurred earlier.

Most of the performance reduction was apparently caused by changes in the facet angles of the individual mirror strips. Some mirror movement resulted from debonding, but most was apparently due to dimensional changes in the flexible polyurethane substrate.

Thermal losses, considered on the basis of loss per unit collector aperture, were relatively high because of the relatively low concentration ratio. The relatively wide receiver aperture also contributed to the thermal loss by providing more area for radiation loss. Providing a hard vacuum in the receiver could reduce the magnitude of thermal losses.

Every solar collector tested at the CMTF has suffered losses in efficiency because of some amount of scattered light from the mirror structure. Those using small mirror facets have had the largest losses because of the difficulty of positioning a large number of facets at precise angles on an economically feasible structure. The FMC Fresnel belt has the additional problem of obtaining a flexible substrate that will remain dimensionally stable during long periods of exposure to the outdoor environment. The design of the unit tested did not achieve the required long term stability.

References

1. Solar Total Energy Program Plan, SAND76-0167 (Revised) Sandia Laboratories, Albuquerque, NM August 1976.
2. FMC Fresnel-Belt Solar Collector Development, SAND78-7037, Sandia Laboratories, Albuquerque, NM July 1979.
3. Therminol 66, Technical Data Sheet, IC/FF-35, Monsanto Company.

Distribution
TID-4500-R66,UC62(268)

Aerospace Corporation
101 Continental Blvd.
El Segundo, CA 90245
Attn: Elliott L. Katz

Acurex Aerotherm
485 Clyde Avenue
Mountain View, CA 94042
Attn: G. J. Neuner

American Technological Univ.
Solar Total Energy Program
P.O. Box 1416
Killeen, TX 76541
Attn: B. L. Hale

Argonne National Laboratory (3)
9700 South Cass Avenue
Argonne, IL 60439
Attn: R. G. Matlock
W. W. Schertz
Roland Winston

Atlantic Richfield Co.
515 South Flower Street
Los Angeles, CA 90071
Attn: H. R. Blieden

Barber Nichols Engineering
6325 W. 55th Avenue
Arvada, CO 80002
Attn: R. G. Olander

Battelle Memorial Institute
Pacific Northwest Laboratory
P.O. Box 999
Richland, WA 99352
Attn: K. Drumheller

Brookhaven National Laboratory
Associated Universities, Inc.
Upton, LI, NY 11973
Attn: J. Blewett

Centro De Fisica da Materia Condensada
Av. Prof. Gama Pinto, 2
1.699 Lisbòa Codex
Portugal
Attn: Manuel Collares Pereira

Congressional Research Service
Library of Congress
Washington, DC 20540
Attn: H. Bullis

Del Manufacturing Co.
905 Monterey Pass Road
Monterey Park, CA 91754
Attn: M. M. Delgado

Desert Research Institute
Energy Systems Laboratory
1500 Buchanan Blvd.
Boulder City, NV 89005
Attn: Jerry O. Bradley

DSET
Black Canyon Stage
P.O. Box 195
Phoenix, AZ 85029
Attn: Gene A. Zerlaut

Honorable Pete V. Domenici
Room 405
Russell Senate Office Bldg.
Washington, DC 20510

Edison Electric Institute
90 Park Avenue
New York, NY 10016
Attn: L. O. Elsaesser

Energy Institute
1700 Las Lomas
Albuquerque, NM 87131
Attn: T. T. Shishman

EPRI
3412 Hillview Avenue
Palo Alto, CA 94303
Attn: J. E. Bigger

General Atomic
P.O. Box 81608
San Diego, CA 92138
Attn: Alan Schwartz

General Electric Company
Valley Forge Space Center
Valley Forge, PA 19087
Attn: Walt Pijawka

General Electric Company
P.O. Box 8661
Philadelphia, PA 19101
Attn: A. J. Poche

Georgia Institute of Technology
School of Mechanical Engineering
Atlanta, GA 30332
Attn: S. Peter Kezios
President
American Society of
Mechanical Engineers

Georgia Institute of Technology
Atlanta, GA 30332
Attn: J. D. Walton

Georgia Power Company
Atlanta, GA 30302
Attn: Mr. Walter Hensley
Vice President
Economics Services

Gruman Corporation
4175 Veterans Memorial Highway
Ro nkonkoma, NY 11779
Attn: Ed Diamond

Hexcel
11711 Dublin Blvd.
Dublin, CA 94566
Attn: George P. Branch

Industrial Energy Control Corp.
118 Broadway
Hillsdale, NJ 07675
Attn: Peter Groome

Jet Propulsion Laboratory
4800 Oak Grove Drive
Pasadena, CA 91103
Attn: V. C. Truscello

Kingston Industries Corp.
205 Lexington Avenue
New York, NY 10016
Attn: Ken Brandt

Lawrence Berkley Laboratory
University of California
Berkley, CA 94720
Attn: Mike Wallig

Distribution (Cont)

Lawrence Livermore Laboratory
University of California
P.O. Box 808
Livermore, CA 94500
Attn: W. C. Dickinson

Los Alamos Scientific Lab (3)
Los Alamos, NM 87545
Attn: J. D. Balcomb
C. D. Bankston
D. P. Grimmer

Honorable Manuel Lujan
1324 Longworth Building
Washington, DC 20515

Mann-Russell Electronics Inc.
1401 Thorne Road
Tacoma, WA 98421
Attn: G. R. Russell

Martin Marietta Aerospace
P.O. Box 179
Denver, CO 80201
Attn: R. C. Rozycki

McDonnell Douglas Astronautics Co.
5301 Bolsa Avenue
Huntington Beach, CA 92647
Attn: Don Steinmeyer

NASA-Lewis Research Center
Cleveland, OH 44135
Attn: R. Hyland

New Mexico State University
Solar Energy Department
Las Cruses, NM 88001

Oak Ridge Associated Universities
P.O. Box 117
Oak Ridge, TN 37830
Attn: A. Roy

Oak Ridge National Laboratory (4)
P.O. Box Y
Oak Ridge, TN 37830
Attn: J. R. Blevins
C. V. Chester
J. Johnson
S. I. Kaplan

Office of Technology Assessment
U.S. Congress
Washington, DC 20510
Attn: Dr. Henry Kelly

Omnium G (2)
1815 Oragethorpe Park
Anaheim, CA 92801
Attn: Ron Derby
S. P. Lazzara

PRC Energy Analysis Company
7600 Old Springhouse Road
McLean, VA 22102
Attn: K. T. Cherian

Rocket Research Company
York Center
Redmond, WA 98052
Attn: R. J. Stryer

Honorable Harold Runnels
1535 Longworth Building
Washington, DC 20515

Honorable Harrison H. Schmitt
Room 1251
Dirksen Senate Office Bldg.
Washington, DC 20510

Scientific Atlanta, Inc.
3845 Pleasantdale Road
Atlanta, GA 30340
Attn: Andrew L. Blackshaw

Sensor Technology, Inc.
21012 Lassen Street
Chatsworth, CA 91311
Attn: Irwin Rubin

Solar Energy Research Institute (9)
1536 Cole Blvd.
Golden, CO 80401
Attn: C. J. Bishop
Ken Brown
B. L. Butler
M. Cotton
R. Gee - D. Kearney
B. P. Gupta
Frank Kreith
A. Rabl

Solar Energy Technology
Rocketdyne Division
6633 Canoga Avenue
Canoga Park, CA 91304
Attn: J. M. Friefeld

Solar Kinetics, Inc.
P.O. Box 10764
Dallas, TX 75207
Attn: Gus Hutchison

Southwest Research Institute
P.O. Box 28510
San Antonio, TX 78284
Attn: Danny M. Deffenbaugh

Stanford Research Institute
Menol Park, CA 94025
Attn: Arthur J. Slemmons

Stone & Webster
Box 5406
Denver, CO 80217
Attn: V. O. Stuab

Sun Gas Company
Suite 800, 2 No. Pk. E.
Dallas, TX 75231
Attn: R. C. Clark

Sundstrand Electric Power
4747 Harrison Avenue
Rockford, IL 61101
Attn: A. W. Adam

Sunsearch, Inc.
669 Boston Post Road
Guilford, CT 06437
Attn: E. M. Barber, Jr.

Suntec Systems, Inc.
2101 Wooddale Dr.
St. Paul, MN 55119
Attn: J. H. Davison

Swedlon, Inc.
12111 Western Avenue
Garden Grove, CA 92645
Attn: E. Nixon

Distribution (Cont)

TEAM, Inc.
8136 Ola Keene Mill Road
Springfield, VA 22151

U. S. Department of Energy (2)
Agricultural & Industrial Process Heat
Conservation & Solar Application
Washington, DC 20545
Attn: W. W. Auer
J. Dollard

U. S. Department of Energy (4)
Albuquerque Operations Office
P.O. Box 5400
Albuquerque, NM 87185
Attn: G. Pappas
C. Quinn
J. R. Roder
J. Weisiger

U. S. Department of Energy (7)
Division of Central Solar Technology
Washington, DC 20545
Attn: R. H. Annan
G. W. Coleman
M. U. Gutstein
G. M. Kaplan
Lou Melamed
J. E. Rannels

U. S. Department of Energy
Los Angeles Operations Office
350 S. Figueroa Street
Suite 285
Los Angeles, CA 90071
Attn: Fred A. Blaski

U. S. Department of Energy
San Franciso Operations Office
1333 Broadway, Wells Fargo Bldg.
Oakland, CA 94612
Attn: Jack Blasy

University of Delaware
Institute of Energy Conservation
Newark, DE 19711
Attn: K. W. Boer

Watt Engineering Ltd.
RR1, Box 183 1/2
Cedaredge, CO 81413
Attn: A. D. Watt

Western Control Systems
13640 Silver Lake Drive
Poway, CA 92064
Attn: L. P. Cappiello

Westinghouse Electric Corp
P.O. Box 10864
Pittsburgh, PA 15236
Attn: J. Buggy

1500 W. A. Gardner
1550 F. W. Neilson
2300 J. C. King
3161 J. E. Mitchell
3600 R. W. Hunnicutt
Attn: 3640 H. H. Pastorius
3700 J. C. Strassell
4000 A. Narath
4531 J. H. Renken
4700 J. H. Scott
4710 G. E. Brandvold
4720 V. L. Dugan
4721 J. V. Otts (213)
4722 J. F. Banas
4723 W. P. Schimmel
4725 J. A. Leonard
4730 H. M. Stoller
5512 H. C. Hardee
5520 T. B. Lane
5600 D. B. Shuster
5834 D. M. Mattox
Attn: 5831 N. J. Magnani
5840 H. J. Saxton
Attn: 5810 R. G. Kepler
5820 R. L. Schwoebel
5830 M. J. Davis
5844 F. P. Gerstle
Attn: 5842 J. N. Sweet
5846 E. K. Beauchamp
8100 L. Gutierrez
8450 R. C. Waybe
8266 E. A. Aas
8470 C. S. Selvage
9572 L. G. Rainhart
3141 T. L. Werner (5)
3151 W. L. Garner (3)
For DOE/TIC
(Unlimited Release)